10-28-2019

Numerical Investigation of Wind Turbine Airfoils under Clean and Dusty Air Conditions

Siyuan Chen
Washington University in St. Louis

Ramesh K. Agarwal
Washington University in St. Louis

Numerical Investigation of Wind Turbine Airfoils under Clean and Dusty Air Conditions

Siyuan Chen[1], Ramesh K. Agarwal[2]
Washington University in St. Louis, St. Louis, MO 63130

This paper focuses on the simulation of the airflow around wind turbine airfoils (S809 and S814) under both clean and dusty air conditions by using Computational Fluid Dynamics (CFD). The physical geometries of the airfoils and the meshing processes are completed in the ANSYS Mesh package ICEM. The simulation is done by ANSYS FLUENT. For clean air condition, Spalart–Allmaras (SA) model and realizable k-ε model are used. The results are compared with the experimental data to test which model agrees better. For dusty air condition, simulation of the two-phase flow is operated by realizable k-ε model and discrete phase model (DPM) in different concentration of dust particles (1% and 10% in volume). The results are compared with the data of clean air to illustrate the effect of dust contamination on the lift and drag characteristics of the airfoil.

Nomenclature

c_l/C_L=lift coefficient
c_d/C_D=drag coefficient
α=angle of attack/AOA
ρ_{air}=density of air
ρ_p=density of dust particles
μ=viscosity of air
Re=Reynolds number
Ma=Mach number
d_p=diameter of dust particles
$\dot{m}_p$=mass flow rate of particles
Δt=time step
F_{other}=other interaction forces
$\vec{u}_p$=velocity of particles
$\vec{u}$=velocity of airflow

[1]Graduate Student, Computational Fluid Dynamics Laboratory, Dept. of Mechanical Engineering & Materials Science.
[2]William Palm Professor of Engineering, Dept. of Mechanical Engineering & Materials Science, Fellow AIAA.

I. Introduction

Because of environmental concerns related to CO_2 emissions and global warming with use of fossil fuels, there is currently great deal of interest in exploitation of renewable energy sources such as wind energy among others. In the context of wind energy, great deal of research is being conducted on the design of wind turbines and wind farms to extract maximum possible energy from the wind. Optimization of aerodynamic performance of both Horizontal Axis Wind Turbines (HAWT) and Vertical Axis Wind Turbines (VAWT) is being investigated. Several wind turbine airfoils/blades have been analyzed and newer airfoils/blades are being analyzed in the literature. National Renewable Energy Laboratory (NREL) in Colorado has led the effort in this research along with industry and academia.

For HAWT, aerodynamic characteristics of S809 airfoil have been extensively studied in the literature. S-series of airfoils are representative of many horizontal-axis wind-turbine (HAWT) airfoils; S809 is a 21% thick low speed airfoil while S814 airfoil is 24% thick airfoil and there are other S-series of airfoils of different thicknesses and cambers with different lift and drag characteristics. S809 and S814 airfoils have been tested in a wind tunnel at the Delft University on Technology and at Ohio State University and the results have been published [2,3], which are utilized in this paper for comparison with the numerical results. However, there are very few publications that consider the influence of dusty air condition on the aerodynamic performance of wind turbine airfoils. In 2017, Douvi, Margaris and Davaris published a paper on the effect of dusty air effect on the aerodynamic performance of S809 airfoil [5].

The focus of this paper is on the evaluation of the aerodynamic performance of the S809 and S814 airfoils in clean air and dusty air by numerical simulation. Incompressible RANS equations are solved with one-equation SA model and two-equation realizable k-ε model. The discrete phase, which consists of dust particles in this case, is injected into the air flow and its effect is calculated using discrete phase model (DPM) in FLUENT. By comparing the results of clean and dusty air conditions, conclusions about the effects of dusty air condition on the aerodynamic performance of airfoils are drawn.

II. Numerical Method and Validation

A. Physical model and Mesh Process

The geometry models of airfoils are constructed using their coordinate's data in Somers's report [1]. The chord lengths of both airfoils are taken to be 1m. As shown in Figs. 2 and 4, the computational domain consists of a semi-circle with radius 25m and a rectangle with 50m height and 25m width. The airfoil is located at the center of the domain. Due to the turbulent boundary layer effects on the flow field near the airfoil, mesh in this region is much denser than the mesh in the far field. ICEM is used for mesh generation. Figure 5 demonstrates that the mesh is of high quality and is adequate for simulation. The solutions are performed on a series of meshes and it is ensured that the solution is mesh independent and the distance of first grid point from the airfoil surface y+ is less than 1.

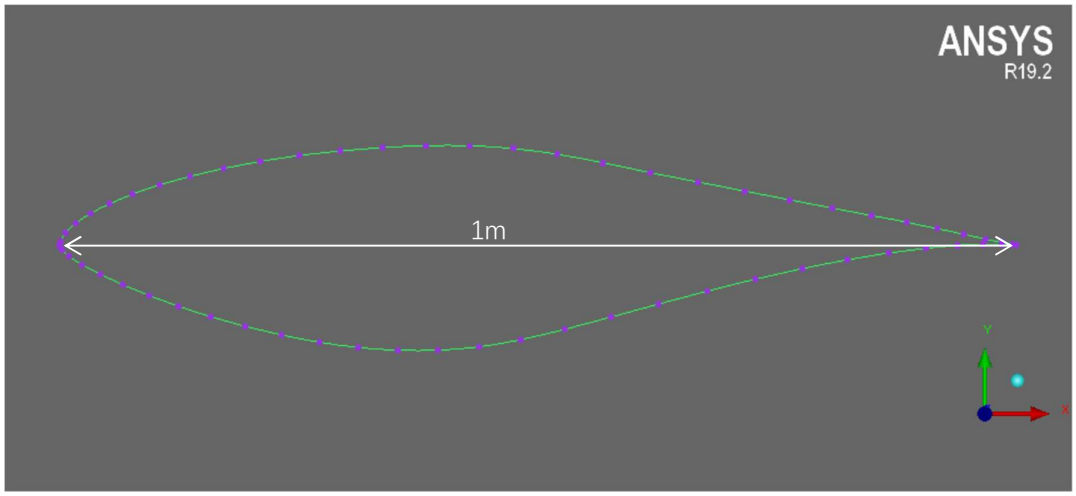

(a) S809 airfoil

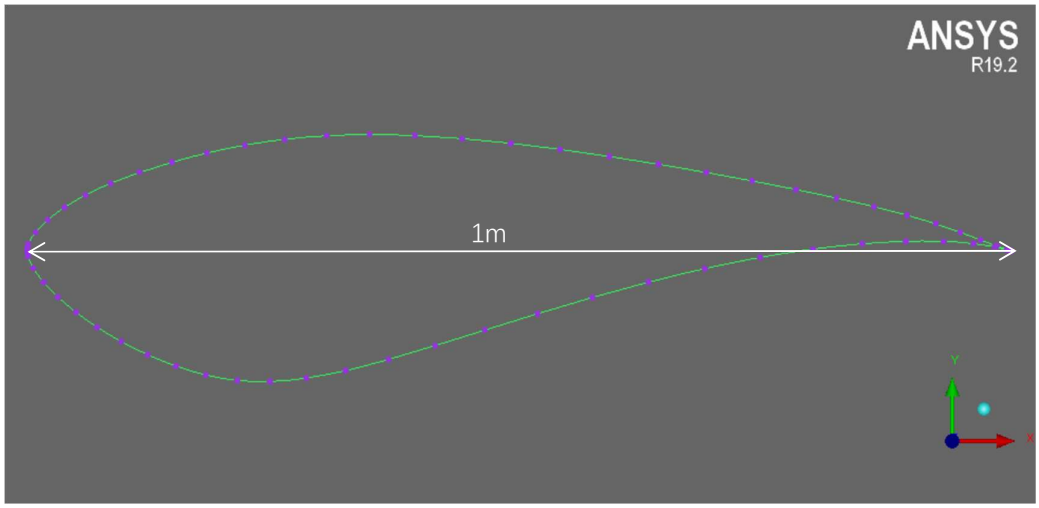

(b) S814 airfoil

Fig.1 Physical models of airfoils

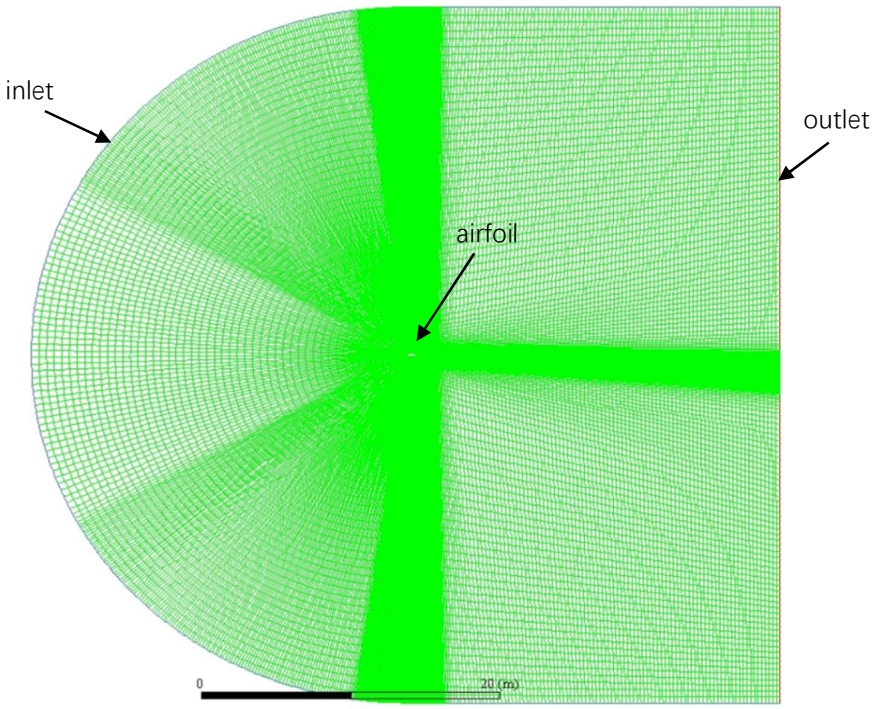

Fig.2 Computational domain and mesh around S809 airfoil

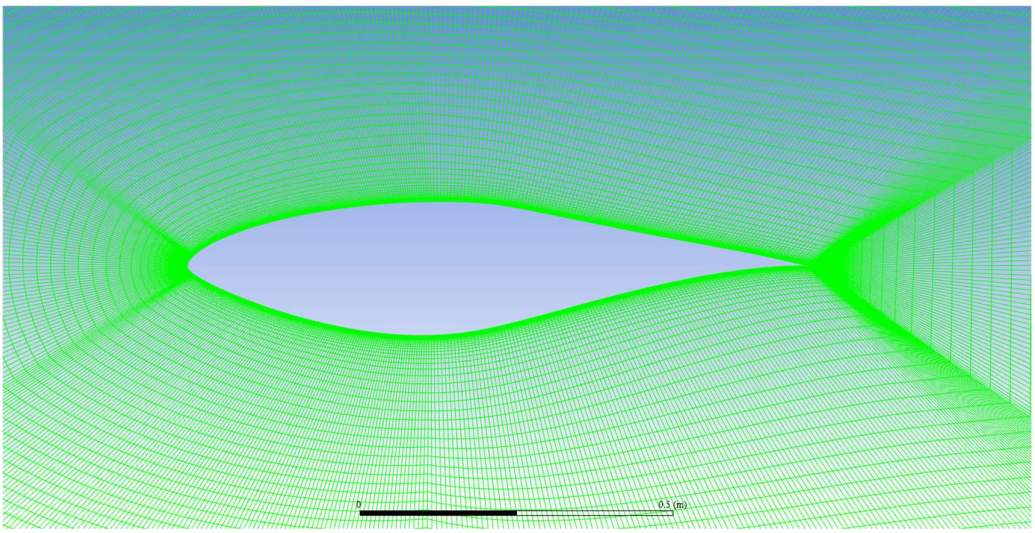

(a) Zoomed-in-view of mesh near S809 airfoil

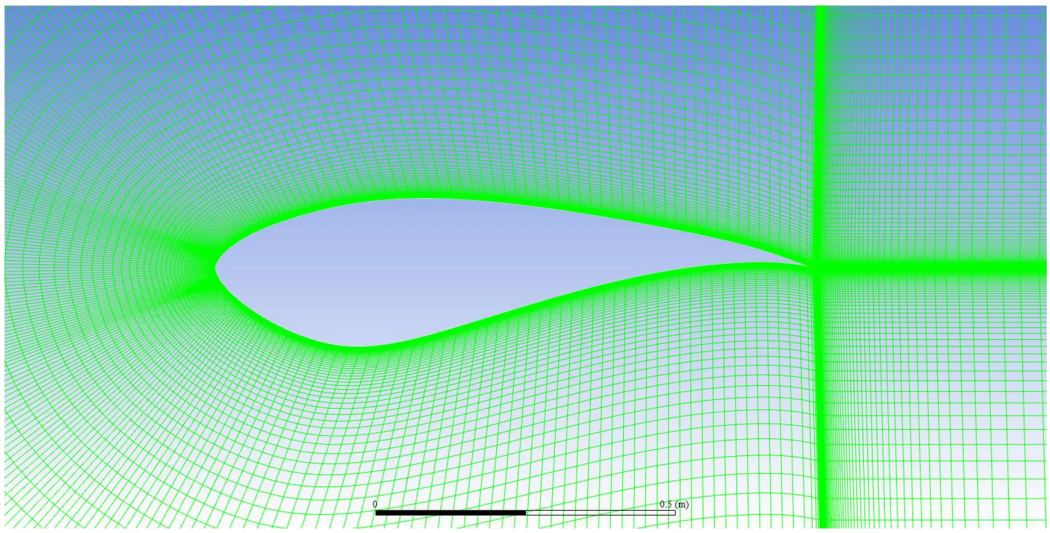

(b) Zoomed-in-view of mesh near S814 airfoil

Fig.3 Zoomed-in-view of mesh near S809 and S814 airfoils

Fig.4 Scale of the mesh

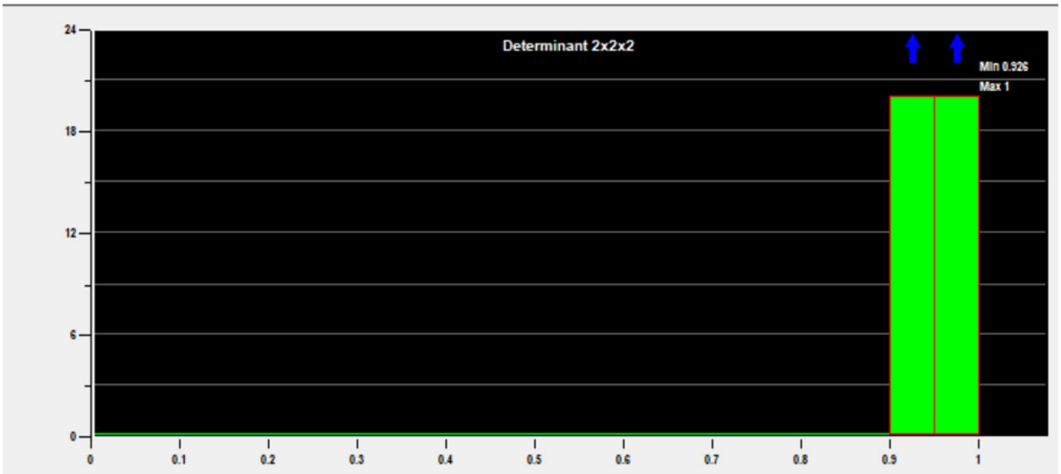

Fig.5 Pre-mesh quality under determinant 2*2*2 criterion

B. Numerical methods and turbulence model

Double precision, pressure-based solver in ANSYS FLUENT is chosen for simulations. For clean air simulation, both SA model [10] and realizable k-ε turbulence model are used with the incompressible RANS equations. All the model constants are kept as "default" values in the code. For dusty air simulation, realizable k-ε model is chosen and the discrete phase model (DPM) in FLUENT is employed to inject the dust particles into the flow field. Coupled scheme for velocity/pressure coupling is chosen for solutions of both clean and dusty air conditions.

C. Discrete phase model (DPM)

Currently there are two numerical methods for calculation of multiphase flows: the Euler-Lagrange approach and the Euler-Euler approach. In the Eulerian-Eulerian approach, the different phases are treated mathematically as interpenetrating continua. Since the volume of a phase cannot be occupied by the other phases, the concept of phase volume fraction is introduced. These volume fractions are assumed to be continuous functions of space and time and their sum is equal to one. In Eulerian-Lagrangian approach, the fluid phase is treated as a continuum by solving the time-averaged Navier-Stokes equations, while the dispersed phase is solved by tracking a large number of particles, bubbles, or droplets through the calculated flow field. The dispersed phase can exchange momentum, mass, and energy with the fluid phase[9]. The change in momentum of a sand particle through each control volume can be calculated by the following equation:

$$\mathrm{F} = \sum \left(\frac{18\mu C_D Re}{24\rho_p d_p^2}\left(u_p - u\right) + F_{oth} \right) \dot{m}_p \Delta t \tag{1}$$

The integration of the force balance on the particle predicts the trajectory of a discrete phase particle[10]. The force balance is written in a Lagrangian reference frame. The forces acting on the particle are equal to the particle inertia and, particularly in the x direction, this equality can be expressed as:

$$\frac{du_p}{dt} = F_d\left(\vec{u} - \vec{u}_p\right) + \frac{\vec{g}}{\rho_p}\left(\rho_p - \rho\right) + \vec{F} \tag{2}$$

$$F_d = \frac{18\mu}{\rho_p d_p^2} \cdot \frac{C_D Re}{24} \tag{3}$$

where $F_D(\vec{u} - \vec{u}_p)$ is the drag force per unit particle mass and $\vec{F}$ is an additional acceleration term, also the force per unit particle mass. Re is the relative Reynolds number, which is defined as

$$\mathrm{Re} \equiv \frac{\rho d_p |\vec{u}_p - \vec{u}|}{\mu} \tag{4}$$

Since the flow is regarded as incompressible and the temperature effects are very small, the energy equation is not considered. For setting the parameters in DPM, surface injection is chosen which means that the dust particles are released into the domain from the inlet surface of the computational domain and escape from the outlet surface of the computational domain. The particles are considered inert. The diameter of the particles is 0.001m and the distribution is considered uniform without any agglomeration. The velocity of the particles is the same as the velocity of the air flow. The density of sand particles is ρp = 1500kg/m3. The free stream temperature is 300K, same as the environmental temperature.

III. Results and Discussion

A. Initial condition of the air flow

In all cases considered, the Reynolds Number of the airflow is $Re=1.5\times10^6$. According to the formula,

$$Re = \frac{\rho \cdot V \cdot d}{\mu}$$

with the density of air $\rho_{air}=1.176674$ kg/m^3 and the viscosity of air $\mu=1.7894\times10^{-5}$kg/m·s, the velocity at the inlet is 22.8m/s and the Mach Number is 0.066.

B. Pressure and velocity contours around airfoils at different angle of attack

Figure 6 and Fig. 7 show the pressure and velocity contours respectively around S809 airfoil at various angles of attack while Fig. 8 and Fig. 9 show the pressure and velocity contours respectively around S814 airfoil at various angles of attack. From the velocity contours, it can be seen that the larger camber near the trailing edge region at the lower surface of the S814 airfoil can create a very low velocity region that can induce separation as the angle of attack increases. Such a behavior of the velocity field affects the pressure field which reduces the lift and increase the drag [6].

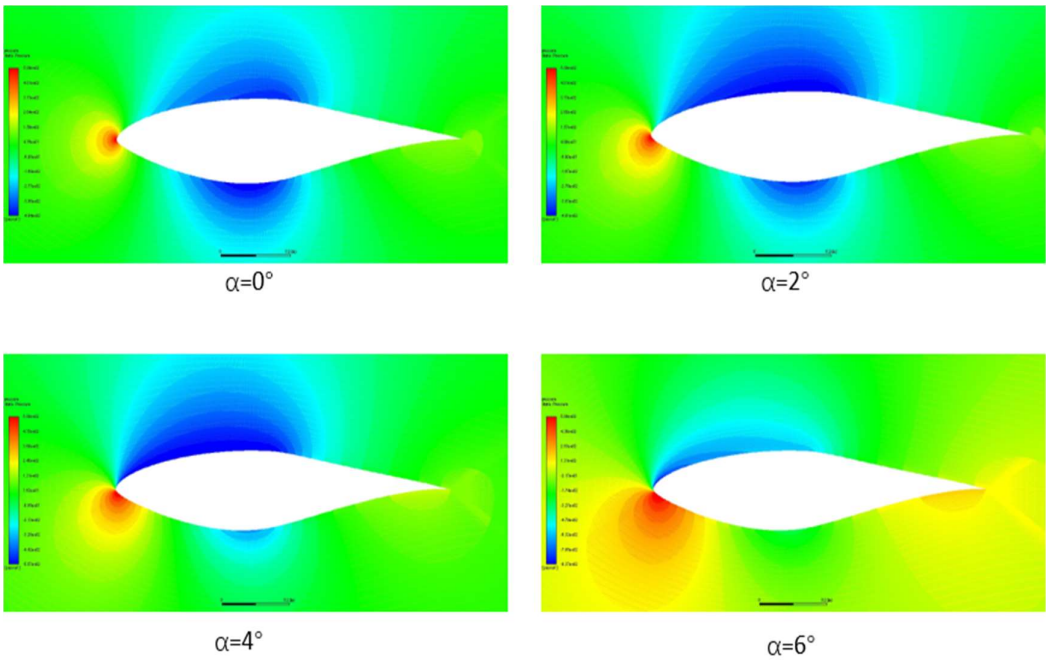

Fig.6 Pressure contours around S809 airfoil under different AOA

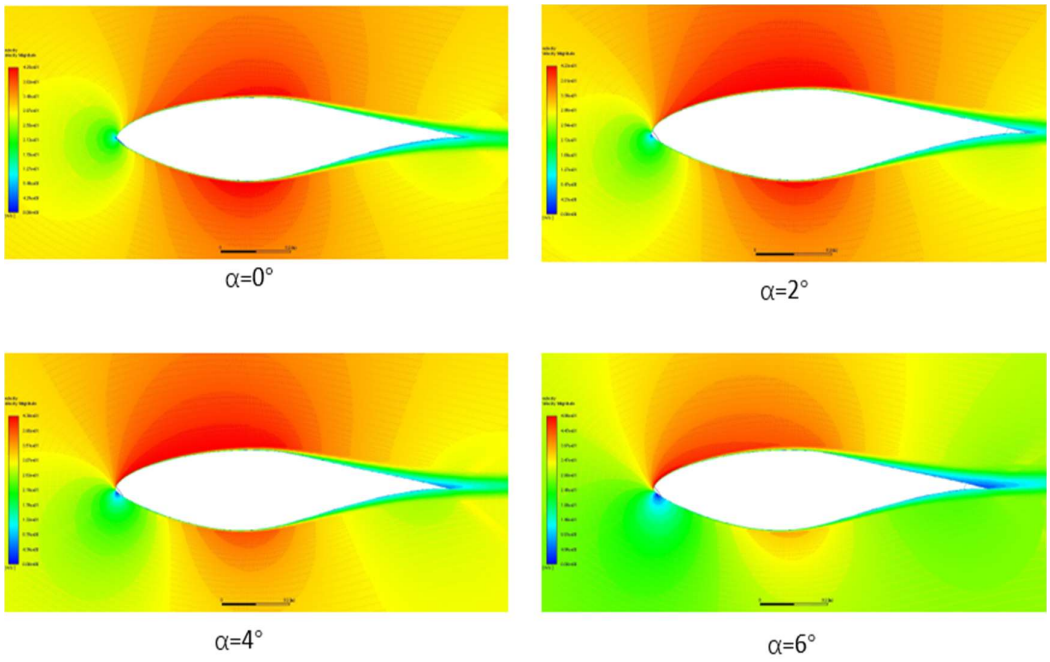

Fig.7 Velocity contours around S809 airfoil under different AOA

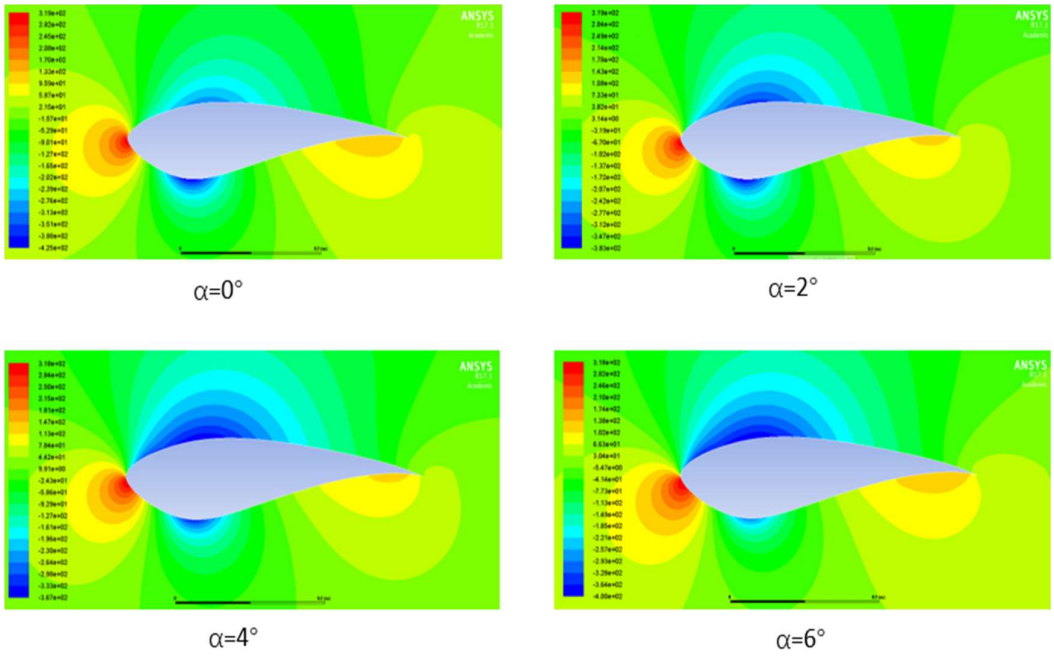

Fig.8 Pressure contours around S814 airfoil under different AOA

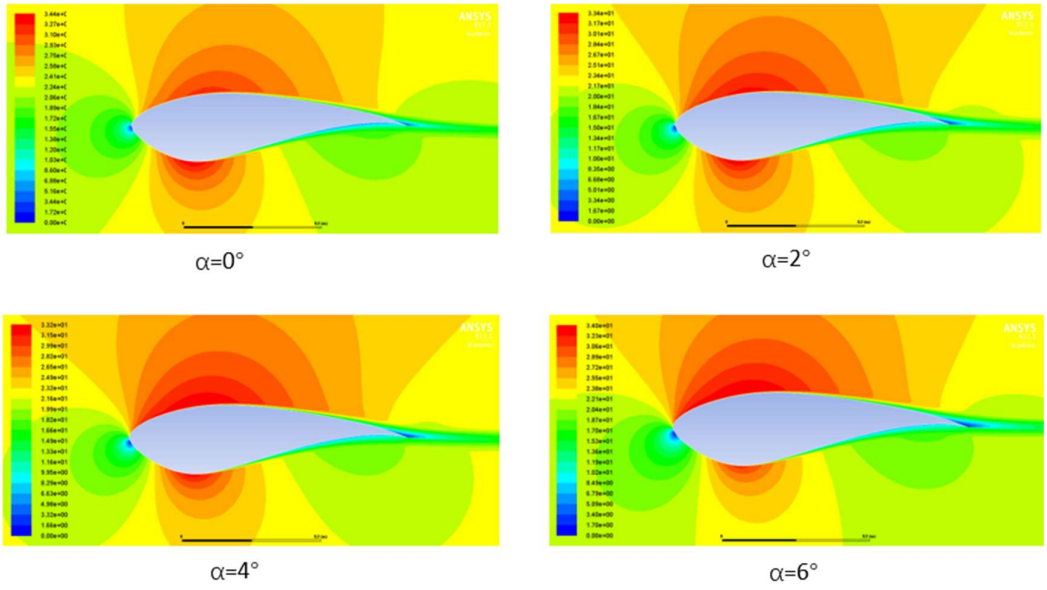

Fig.9 Velocity contours around S814 airfoil under different AOA

C. Results for S809 airfoil at different Reynolds Number under clean air condition

Since Re and free stream velocity V are linearly dependent with ρ, d and μ being unchanged, different Re means different free stream velocity faced by the airfoil. Figure 10 shows that the lift coefficient increases slightly when the Reynolds number increases from 1×10^6 to 1.5×10^6, which leads to change in lift to drag ratio. This observation has also been mentioned in other papers [7].

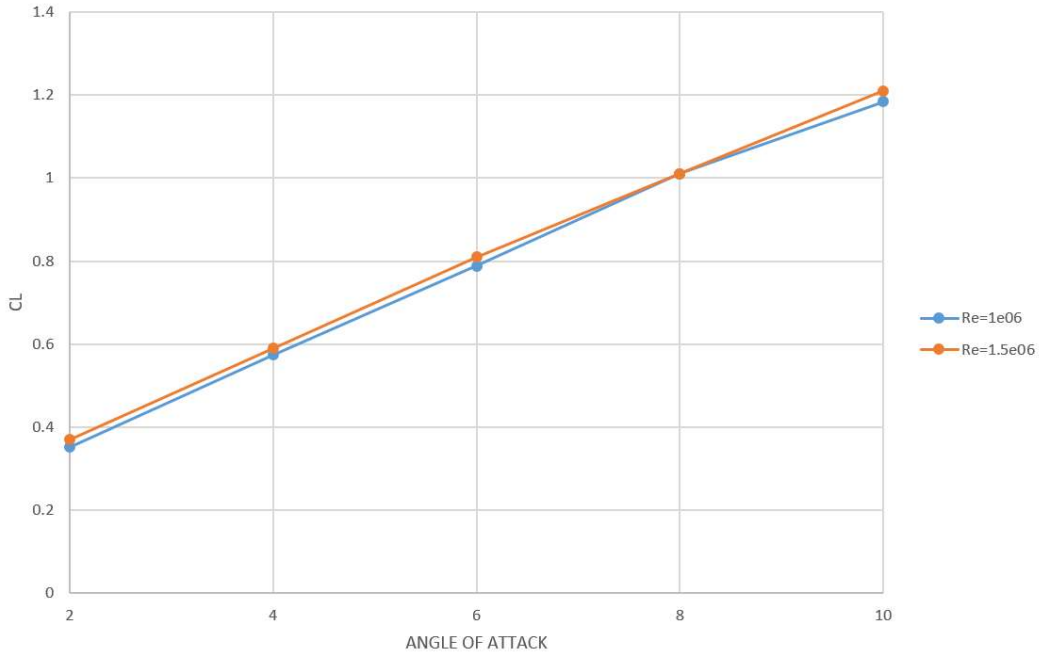

Fig. 10 Variation in lift coefficient of S809 airfoil with angle of attack at two Reynolds Numbers

D. Results of clean air past S809 and S814 airfoils using the SA and realizable k-ε models and comparison with experimental data

Figures 11 and 12 show computed results for the two airfoils using SA and realizable k-ε model and their comparison with the experimental data given in [4, 11]. For S809 airfoil, both models show very good agreement with the experimental data for some range of AOA; however results using realizable k-ε model show better agreement with the data. For S814 airfoil, only realizable k-ε model is employed and the agreement is not as good as for the S809 airfoil. It can be observed that cl is linearly dependent on AOA when α is small. As α increases, linearly dependence no longer exists and the computed results are significantly different from the experimental data due to the effect of stall [8]. One more interesting fact is that the cl-α curve does not pass through the origin, which means that non-zero lift force exists when angle of attack is zero; it is expected since the airfoil is not completely symmetrical and this asymmetry results in pressure difference between upper and lower part of the airfoil [6]. Furthermore, from Fig. 13, it can be seen that S814 airfoil has larger lift coefficient than S809 airfoil at same angle of attack due to larger camber. Thus S814 airfoil has better aerodynamic performance. The can be easily explained by the geometry in Figure 1. It is obvious that S814 airfoil has higher asymmetry and camber resulting in greater pressure difference between the upper and lower surface of the airfoil, which leads to higher lift coefficient [12].

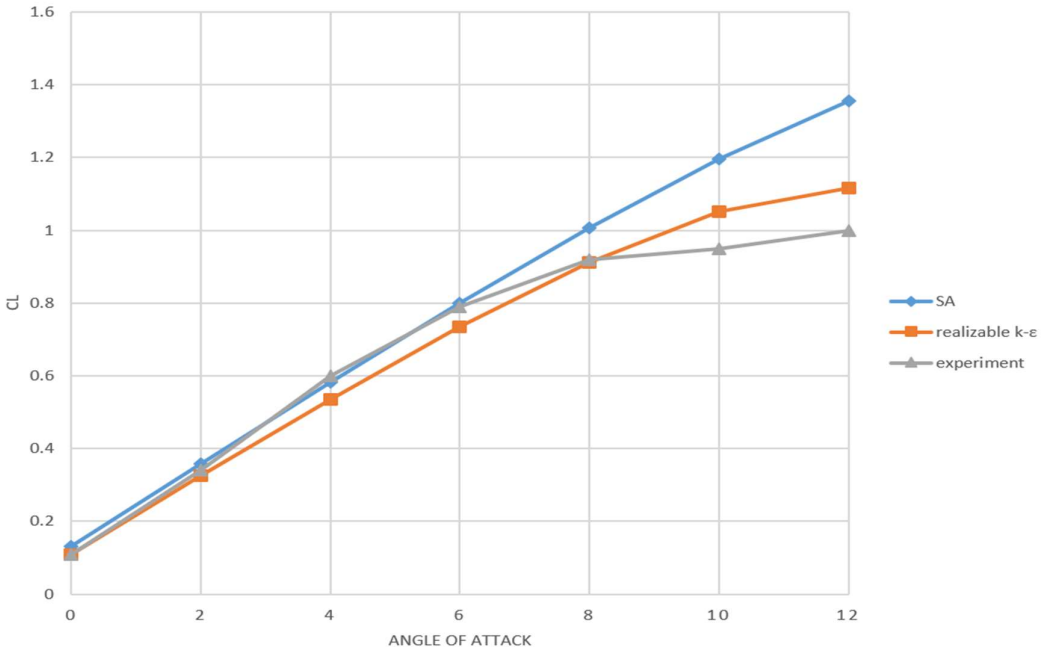

Fig. 11 Variation in lift coefficients of S809 airfoil under clean air condition using SA model, realizable k-ε model and comparison with experimental data

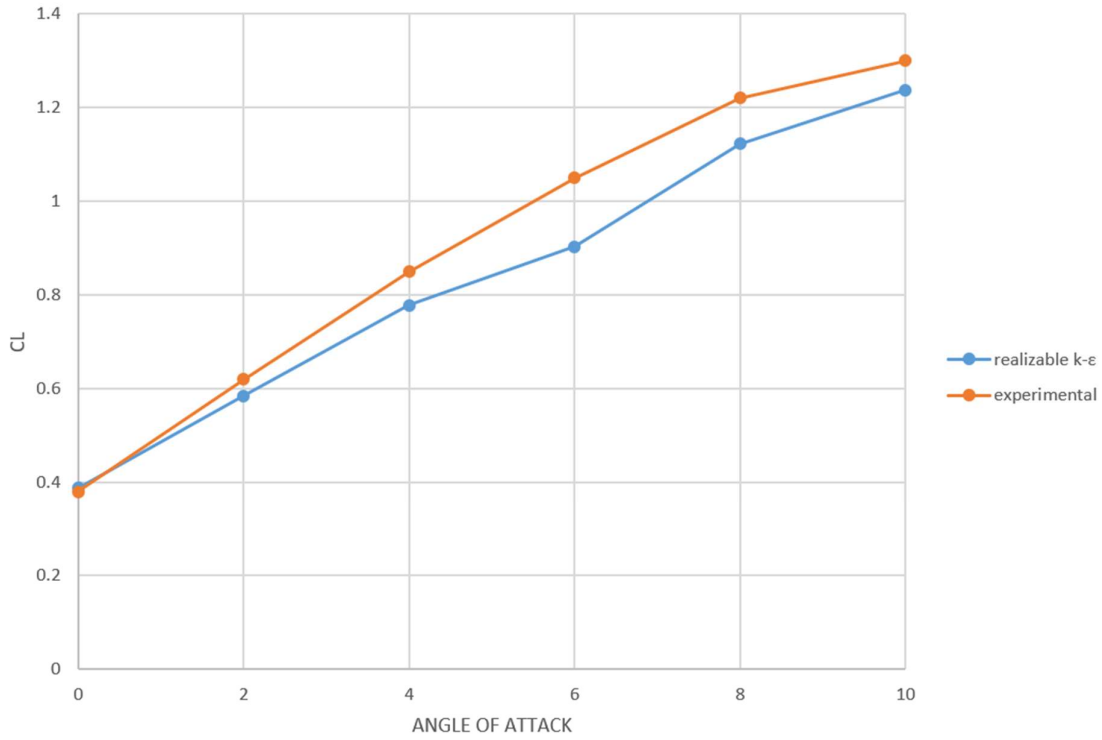

Fig. 12 Variation in lift coefficients of S814 airfoil under clean air condition using SA model, realizable k-ε model and comparison with experimental data

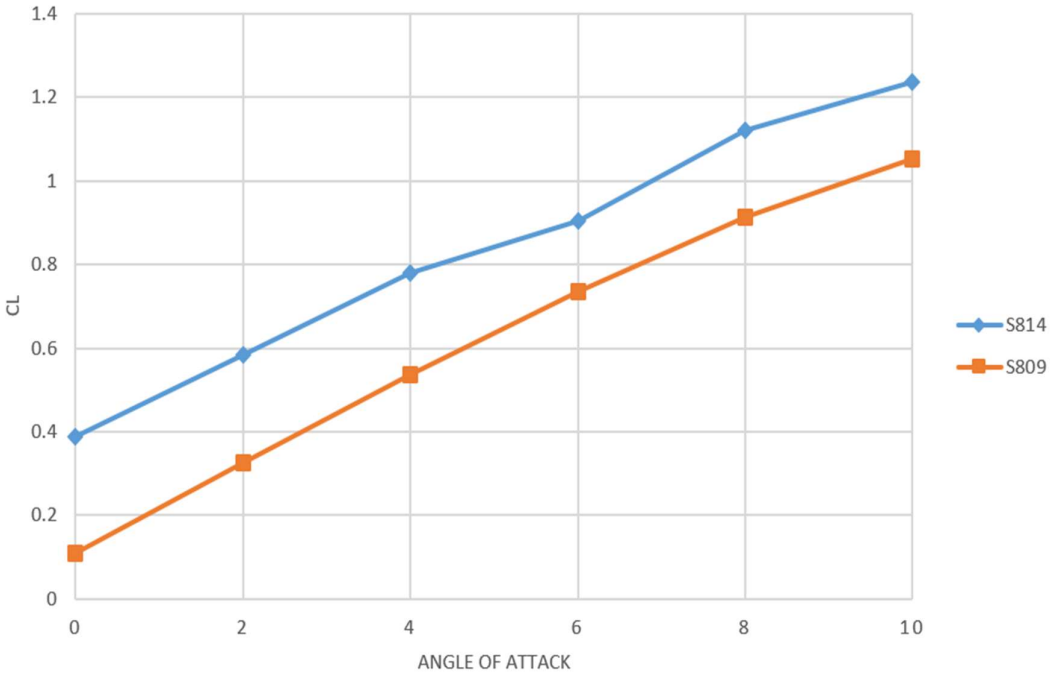

Fig. 13 Comparison of computed lift coefficients of S809 and S814 airfoil under clean air condition using realizable k-ε model

E. Results for dusty air (with sand grains) and their comparison with clean air results

By using realizable k-ε model and discrete phase model, results of dusty air condition are calculated and compared with results of clean air condition. Figure 14 and 15 show the difference in results using clean air and dusty air with 1% and 10% concentration in volume. From these figures, it can be concluded that the aerodynamic characteristics of S809 airfoil will change due to presence of dust particles; the lift coefficient decreases and drag coefficient increases as expected. For 1% particle concentration, the change in aerodynamic coefficients is very small and the results are very close with clean air as expected. However, for 10% concentration, some changes in aerodynamic coefficients can be observed.

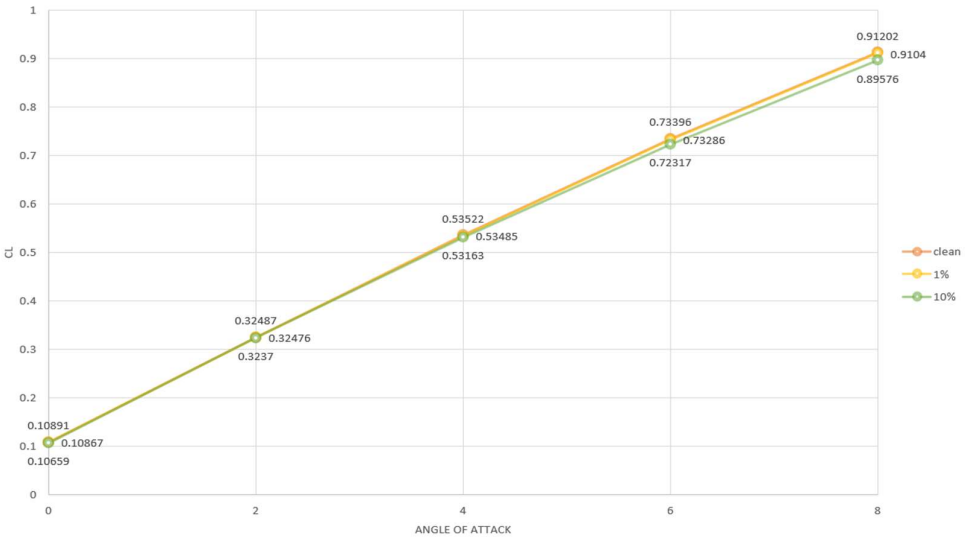

Fig. 14 Change in lift coefficient of S809 airfoil under clean and dusty air conditions

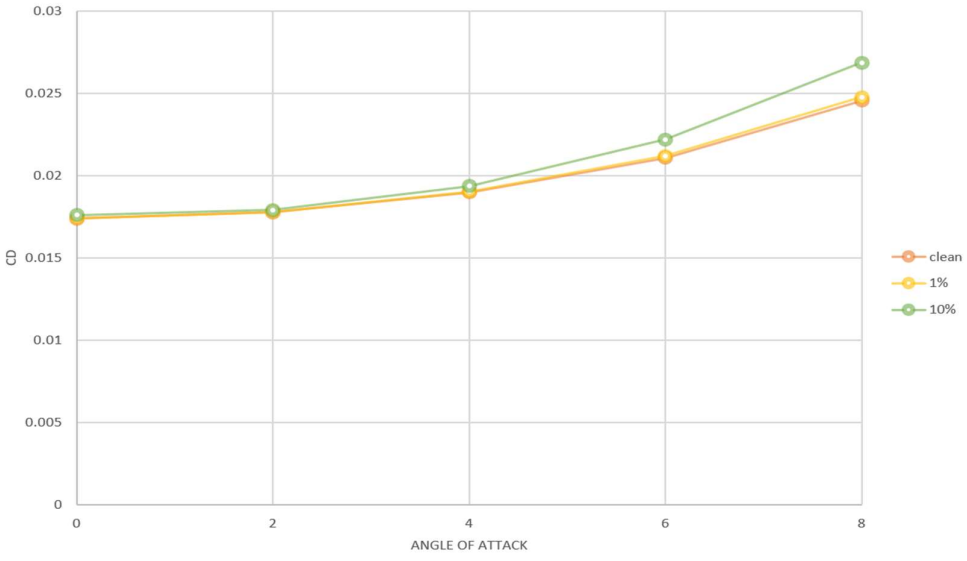

Fig. 15 Change in drag coefficient of S809 airfoil under clean and dusty air conditions

IV. Conclusions

Several conclusions can be drawn based on this research:

1. Aerodynamic performance of wind turbine airfoils is influenced by the usual flow and geometric parameters such as angle of attack, Reynolds number, thickness and camber as well as by conditions of air (clean or dusty).
2. Injection of dust particles can generate negative effects on the aerodynamic performance of the wind turbine airfoil; the drag coefficient increases and the lift coefficient decreases resulting in a lower lift to drag ratio.
3. Based on the comparison between results of 1% and 10% concentration of particles by volume in dusty air, it is found that larger concentration of dust particles has more detrimental effects on aerodynamic performance as expected and therefore on the power output of the wind turbine.
4. The wind turbines will not only have erosion and degradation of blades in dusty environment but also poor power generation in countries where sand dust is very common in the environment e.g. countries in the Middle East.

V. References

[1] Walter P. Wolfe, Stuart S. Ochs, "CFD Calculation of S809 Aerodynamic Characteristics", Office of Scientific and Technical Information (OSTI), October 1996.

[2] Dan M. Somers, "Design and Experimental Results for the S809 Airfoil," National Renewable Energy Laboratory, January 1997.

[3] Dan M. Somers, "Design and Experimental Results for the S814 Airfoil," National Renewable Energy Laboratory, January 1997.

[4] R. Reuss Ramsay, M. J. Hoffmann, G.M. Gregorek "Effects of Grit Roughness and Pitch Oscillations on the S809 Airfoil," National Renewable Energy Laboratory, December 1995.

[5] Dimitra C. Douvi, Dionissios P. Margaris, Aristeidis E. Davaris, "Aerodynamic Performance of a NREL S809 Airfoil in an Air-Sand Particle Two-Phase Flow", MDPI, February 2017.

[6] John D. Anderson, Jr. "Fundamentals of Aerodynamics" Sixth Edition, University of Maryland, McGraw-Hill Education, 2017..

[7] Shubham Jain, Nekkanti Sitaram, Sriram Krishnaswamy, "Effect of Reynolds Number on Aerodynamics of Airfoil with Gurney Flap", Hindawi Publishing Corporation, International Journal of Rotating Machinery Volume 2015.

[8] M.J. Barnsley and J.F. Wellicome, "Wind tunnel investigation of stall aerodynamics for a 1.0 m horizontal axis rotor", Journal of Wind Engineering and Industrial Aerodynamics, 1992

[9] Tung Wan, Szu-Peng Pan, "Aerodynamic Efficiency Study Under the Influence of Heavy Rain via Two-Phase Flow Approach", 27th international congress of the aeronautical sciences, 2010

[10] P. R. Spalart, S. R. Allmaras, "A One -Equation Turbulence Model for Aerodynamic Flows", AIAA 30th Aerospace Sciences Meeting and Exhibit, January 1992

[11] R. Reuss Ramsay, M. J. Hoffmann, G.M. Gregorek "Effects of Grit Roughness and Pitch Oscillations on the S814 Airfoil," National Renewable Energy Laboratory, May 1996.

[12] Justin Winslow, Hikaru Otsuka, Bharath Govindarajan, and Inderjit Chopra "Basic Understanding of Airfoil Characteristics at Low Reynolds Numbers (10^4–10^5)", University of Maryland, Journal of Aircraft, Vol. 55, No. 3, May–June 2018.